Received: 8 April 2022 | Revised: 2 July 2022 | Accepted: 11 July 2022

DOI: 10.1002/met.2087

Meteorological Applications
Science and Technology for Weather and Climate
Open Access
RMetS

RESEARCH ARTICLE

A review of early severe weather applications of high-resolution regional reanalysis in Australia

Paul Fox-Hughes[1] | **Chun-Hsu Su**[2] | **Nathan Eizenberg**[3] | **Christopher White**[4] | **Peter Steinle**[2] | **Doerte Jakob**[2] | **Mitchell Black**[2] | **Andrew Dowdy**[2] | **Andrew Brown**[3] | **Rory Nathan**[5] | **Suwash Chandra Acharya**[5]

[1]Research Program, Australian Bureau of Meteorology, Hobart, Tasmania, Australia

[2]Research Program, Australian Bureau of Meteorology, Melbourne, Victoria, Australia

[3]School of Geography, Earth and Atmospheric Sciences, University of Melbourne, Parkville, Victoria, Australia

[4]Centre for Water, Environment, Sustainability and Public Health, University of Strathclyde, Glasgow, UK

[5]Department of Infrastructure Engineering, University of Melbourne, Parkville, Victoria, Australia

Correspondence
Paul Fox-Hughes, Research Program, Australian Bureau of Meteorology, GPO Box 727, Hobart, TAS 7001, Australia.
Email: paul.fox-hughes@bom.gov.au

Funding information
New South Wales Rural Fire Service; South Australian Country Fire Service; South Australian Department of Environment and Water; Tasmanian and Australian Governments; West Australian Department of Fire and Emergency Services; University of Tasmania; Antarctic Climate and Ecosystems Co-operative Research Centre

Abstract

High-resolution regional reanalysis datasets have the potential to provide valuable guidance to emergency management agencies, highlighting areas at risk of severe weather, including estimates of return periods of various hazardous weather phenomena. The BARRA regional reanalysis for Australia comprises a reanalysis for a broad region around Australia at moderately high spatial and temporal resolution (12 km/hourly), together with four subdomains at high resolution (1.5 km/1 h). Here, we document four applications of BARRA developed for emergency management: optimal placement of portable automatic weather stations for fire weather monitoring; climatology of low-level wind shear conducive to cool-season tornadogenesis; development of rainfall intensity–frequency–duration curves based on the gridded reanalysis data; and development of a climatology across Australia of parameters associated with severe thunderstorm occurrence.

KEYWORDS

emergency management, reanalysis applications

1 | INTRODUCTION

This paper aims to document a number of applications of the high-resolution reanalysis Bureau of Meteorology Atmospheric high-resolution Regional Reanalysis for Australia (BARRA, Su et al., 2019, 2021), highlighting its potential for both foundational and applied research. BARRA offers the opportunity to study the detailed evolution of significant weather events in the Australian region and to characterize historical hazards, including their frequency, severity and seasonality. The paper will identify limitations of the BARRA reanalysis and illustrate situations in which caution is required in interpretation of results. This information will guide future versions of the reanalysis.

A reanalysis is useful for meteorological studies or for activities that require meteorological data because it is available across an entire spatial domain at high temporal resolution in an internally physically consistent form. In situ weather observations, on the other hand, are generally spatially discrete, are often not available as a complete series and, due to issues of siting and instrumentation, may not offer physical consistency across time at a single observation site, let alone within a network of sites. A reanalysis includes information from observations in the past—Cardinali (2013) concluded that more than 80% of the information in an analysis timestep is derived from previous observations. Further, a reanalysis offers the opportunity to investigate and describe weather parameters that are not easily or frequently observed.

Reanalysis and observational data differ substantially. Reanalysis parameters for a grid cell represent an estimate of parameters over the entirety of the grid cell, which have horizontal dimensions of 1.5 × 1.5 km in the case of BARRA. On the other hand, observations are representative only at the locations at which they are made, although generally observation sites are chosen to ensure that the data are representative of conditions across the surrounding area.

Numerous studies have used reanalysis data, with the paper documenting the ERA-Interim reanalysis (Dee et al., 2011), for example, having been cited more than 21,000 times (as of December 2021, according to Google Scholar). Reanalyses have been used to investigate notable events (Giese et al., 2010; Grumm et al., 2005; Hamill et al., 2005; Ndalila et al., 2020; Neff et al., 2013; Slivinski et al., 2021), or as the boundary conditions for higher resolution weather prediction models investigating historical events in greater detail (Mills, 2005; Stucki et al., 2015, 2018; Senatore et al., 2020). A particularly powerful application lies in examining climatologies and variability of particular types of events (Abatzoglou et al., 2021; Brooks et al., 2003; Manney & Hegglin, 2018; Rodríguez & Bech, 2021; Škerlak et al., 2015).

Reanalyses do, of course, have limitations. Changes in the nature and frequency of underlying observational data have sometimes subtle effects on reanalysis fields (Diniz & Todling, 2020). Errors in assimilated observations can propagate into reanalyses. A reanalysis itself is generated from numerical weather prediction models with the first guess or background fields of the reanalysis derived from the NWP model. Parameterization of, for example, surface weather parameters or cloud microphysical quantities may result in errors or biases in those quantities and in derivative fields. Because of the potential wide utility of reanalyses, it is important to communicate both the strengths and weaknesses of reanalysis data.

While instruments may be calibrated against accurate reference standards, there are no equivalent standard reference datasets for reanalyses. As a result, evaluation of reanalysis accuracy must be made against other reanalysis products or against independent observations, that is, observations not used in the derivation of the reanalysis being assessed. It may therefore be difficult to identify systematic reanalysis errors. Notwithstanding these limitations, many reanalyses continue to be widely used in research and applications that require weather and climate data, as their benefits generally far outweigh the limitations noted and can provide complementary insight to that based directly on observations.

Regional reanalysis projects and datasets have been developed over the last one to two decades as computing resources have become more powerful. Regional reanalyses are attractive to those wishing to use weather and climate data because their limited domains permit higher spatial and temporal resolution than do global reanalyses, given comparable computing resources (Kaiser-Weiss et al., 2019). The North American Regional Reanalysis (NARR, Mesinger et al., 2006), initially for the 25-year period 1979–2003, was the first such product developed. Mesinger et al. (2006) evaluated NARR as being very successful, resolving surface and free atmospheric features (such as jet streams) in greater detail and even better accuracy than had been anticipated. Several other regional reanalyses have followed, including the COSMO regional reanalysis at approximately 6 km horizontal grid spacing over all of Europe (Bollmeyer et al., 2015), and a ∼2.5 km grid spacing convection-permitting reanalysis over Central Europe (Wahl et al., 2017). Individual European nations have also pursued regional reanalysis projects (Gleeson et al., 2017). The Arctic is the subject of a number of specific regional reanalysis efforts, including the Regional Arctic System Reanalysis (Bromwich et al., 2016). More equatorial and arid regions have also been the subject of reanalysis projects, such as the Red Sea and adjacent land areas (Viswanadhapalli et al., 2017). Similarly, the Indian Monsoon Data Assimilation and Analysis reanalysis (IMDAA, Ashrit et al., 2020) has been created to examine the Indian monsoon, while the East Asia Regional Reanalysis is being developed centred on the Korean Peninsula (Yang et al., 2021).

As described more fully in Su et al. (2019, 2020), BARRA is the first regional reanalysis for Australia and the surrounding region. It provides hourly fields of meteorological variables between 1990 and 2018 at approximately 12 km horizontal grid resolution. Currently, four subdomains at 1.5 km horizontal grid resolution have been developed over the same time period, to better resolve smaller-scale features. These were created with support from relevant state fire and emergency services agencies and, in the case of a Tasmanian subdomain, in association with the University of Tasmania.

2 | MODEL SET-UP

BARRA is a regional atmospheric reanalysis developed for the Australasian region (Jakob et al., 2017), covering the 29-year period from 1990 to 2018. It is run at a higher resolution than contemporary global reanalyses such as the widely used ERA-Interim reanalysis (Dee et al., 2011). It is also run at higher resolution than more recent global reanalyses that have been developed since this version of BARRA was first produced, including the current highest resolution (~30 km horizontal grid spacing) global reanalysis ERA5 (Hersbach et al., 2020).

BARRA was produced using two steps, detailed as follows.

The first step is a limited-area reanalysis (BARRA-R) defined on a 12-km horizontal grid covering the Australian continent and its surrounding regions including part of southeast Asia, New Zealand and the Southern Ocean extending to the ice edge of the Antarctic continent (Figure 1). A vertical grid spans from the surface to 80 km above the surface. It is constrained at the boundary in a one-way nesting inside the global reanalysis ERA-Interim. The reanalysis was generated through a sequential time-stepping procedure, consisting of cycles of data assimilation every 6 h, centred on 0000 UTC and successive 6 h increments and numerical model forecasts of 12 h duration. At each of these cycles, the initial condition is determined by iteratively changing a model (initial) state to minimize the difference between its forecasts and the observations. This difference is measured objectively using a cost metric similar to root-mean-square errors. When the minimization converges, the optimized model state is the desired initial condition (known as an analysis). The BARRA data sets are constructed by repeating the model forecasts from a series of these analyses. The specific implementation of the data assimilation system for the atmosphere is 4D variational analysis (4D-Var, Courtier et al., 1994), which matches forecast model states to observations at their proper times. BARRA uses many types of observations in each analysis, including land and ship observations, as well as from aircraft, radiosondes and satellites. Satellite data are particularly important for the Southern Hemisphere, due to lack of other types of observations over large areas of ocean. Altogether, these observations provide information about states and motions of the atmosphere at surface and over different layers.

In the second step, BARRA-R reanalysis was downscaled to finer resolution, again using the BARRA modelling framework but without data assimilation, consistent with the Bureau of Meteorology's approach in nesting operational NWP suites (see Su et al., 2021 for details). This second downscaling step was to a 1.5-km horizontal grid with the model top level at 40 km for four subdomains centred at Perth (BARRA-PH), Adelaide (BARRA-AD), Tasmania (BARRA-TA) and Sydney (BARRA-SY), as shown in Figure 1. Collectively, these very fine-scale datasets are referred to as BARRA-C. Note that the model top level is substantially lower than in BARRA-R, but both models use 70 vertical levels. The higher vertical and horizontal resolution allows BARRA-C to begin to explicitly resolve convective processes and complex orographic flow. Contrary to BARRA-R, BARRA-C is run without a convective parameterization scheme, instead using model dynamics to represent vertical motion and moisture transport between the vertical levels. Further

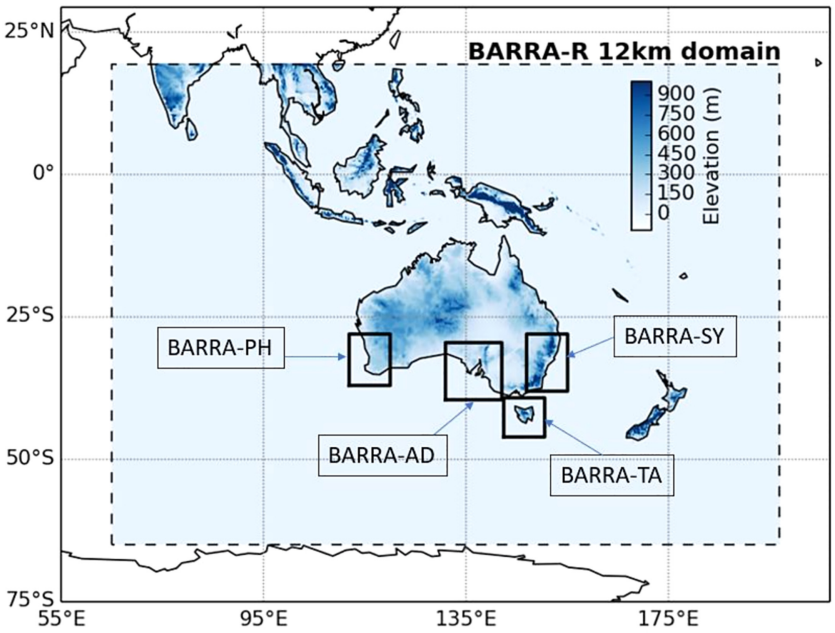

FIGURE 1 BARRA domains: The dotted line represents the boundary of BARRA-R, while the four smaller black boxes show subdomains over southwest Western Australia (BARRA-PH), southeastern South Australia (BARRA-AD), Tasmania (BARRA-TA) and eastern New South Wales (BARRA-SY)

differences in the boundary layer, cloud microphysics and land surface parameterizations are described in Su et al., 2021. The horizontal boundary and 40 km model top conditions of BARRA-C come from hourly BARRA-R output. BARRA-C runs at a smaller spatial and temporal scale than BARRA-R, so any influence of the upper levels of BARRA-R (in the upper stratosphere and above) has been verified in practice to have limited or no impact over the timescales of interest.

The Australian Community Climate and Earth-System Simulator (ACCESS) is the underpinning model used in BARRA and the Bureau of Meteorology's numerical weather prediction (NWP) systems (Bureau of Meteorology, 2018, 2019). ACCESS comprises the UK Met Office Unified Model (UM, Davies et al., 2005) for the atmosphere, and the Joint UK Land Environment Simulator (JULES, Best et al., 2011) for the land surface/subsurface. Similarly, the incremental formulation of the 4D-Var data assimilation scheme of the Met Office (Rawlins et al., 2007) is used in BARRA and the Bureau of Meteorology's NWP.

Su et al. (2019, 2021) provide details and assessments of BARRA-R and BARRA-C, respectively. Both BARRA implementations produce a credible reproduction of near-surface meteorology over land. They improve upon its global driving model ERA-Interim, showing better agreement with finer-scale observational data sets such as in situ observations and gridded analysis for temperature and precipitation. While less pronounced than coarse-scale global reanalyses, biases do exist in BARRA, such as cold (warm) bias in daily maximum (minimum) temperature and negative (positive) bias in 10 m wind during high (low) wind conditions. Inter-annual shifts in biases relative to land observation analyses also exist in BARRA, as with the global reanalyses, possibly due to changes in large-scale climate drivers or changes in observing systems. May et al. (2021) found BARRA is highly correlated with observed moist parameters in northern tropical Australia, despite some seasonally and diurnally varying biases. The wet bulb temperature and dew point temperature have lower uncertainty than nominal temperature.

BARRA-R and BARRA-C are different in a number of aspects. BARRA-C shows better agreement with point observations for temperature and wind in topographically complex and coastal regions. BARRA-C also improves upon BARRA-R in terms of intensity and timing of precipitation and spatial patterns of storm cells during the thunderstorm seasons in NSW. As convective processes are unresolved in BARRA-R, the model has simulated too much light rain and underestimates heavy rain, but can still provide valuable information on daily and sub-daily precipitation (Acharya et al., 2019, 2020). By contrast, BARRA-C has more realistic spatial rainfall distributions and timing but shows overestimation of heavy rain rates and rain cells, and underestimates light rain occurrence. BARRA-C avoids issues with unrealistically strong vertical winds seen in BARRA-R due to instability in the convection parameterization scheme (Su et al., 2019).

As BARRA-C does not assimilate observations, it largely inherits the domain-average bias pattern from BARRA-R. However, it produces different climatological extremes for temperature and precipitation. BARRA-C provides added skill over BARRA-R in terms of capturing spatial patterns of temperature extremes and wet precipitation extremes but remains biased in terms of magnitude.

3 | APPLICATIONS

Applications documented in this paper have an emergency management focus. This is because, as noted above, the emergency management sector were strong early supporters of efforts by the Bureau of Meteorology to develop a reanalysis for the Australian region. The applications documented here include:

1. Cool-season tornadoes in Western Australia
2. Siting of portable Automatic Weather Stations in New South Wales during periods of elevated fire danger
3. Thunderstorm climatology and severe convective weather hazards
4. Derivation of design rainfalls

In each case, the high-resolution reanalysis has a dual value. It provides a spatially and temporally consistent indication of the mean state of the variables of interest. Simultaneously, however, it permits investigation of departures from those mean states. The parameters under investigation vary between cases, but, given the interest of emergency managers, the reanalysis subsets in each application represent extremes of the parameters under investigation. A further advantage of the use of high-resolution reanalyses for emergency management studies is that they represent the state of a wide range of meteorological variables so that, if desired, the same dataset can be queried to explore the influence of multiple parameters or cascading events, for example, cases where antecedent heavy precipitation rendered soils less able to support trees in high winds, resulting in widespread damage due to treefall.

3.1 | Cool-season tornadoes in Western Australia

The southwest coast of Western Australia (WA) is exposed to active frontal weather systems moving across the southern Indian Ocean. It is subject to outbreaks of

cool-season tornadoes within such frontal systems mostly during May–October (Hanstrum et al., 2002), a characteristic common to other regions of southern Australia (Fox-Hughes et al., 1996, 2018; Mills, 2004; Watson, 1985) and other mid-latitude coastal or near-coastal regions with prevailing onshore winds (Clark, 2009; Leitão & Pinto, 2020; Monteverdi & Quadros, 1994; Tyrrell, 2007).

Cool-season tornadoes have been identified as forming in high-shear, often low convective available potential energy (CAPE) environments (Hanstrum et al., 2002). These events can be difficult to forecast (King et al., 2017; Sherburn et al., 2016), so better understanding of their occurrence is valuable. To improve such understanding, reanalysis climatologies of cool-season tornado environments have been developed on a regional or continental scale in the past (Kounkou et al., 2009; Rodriguez & Bech, 2021) and at times on a global scale (Brooks et al., 2003). Geographically comprehensive climatologies using gridded datasets such as this are valuable because observation-based climatologies will never be able to include all locations that may be subject to tornadogenic weather. However, the use of global reanalyses for such climatologies risks missing features at temporal and spatial scales below the resolution of the global reanalysis, as noted above. On the other hand, the BARRA-PH dataset, at 1.5 km horizontal grid resolution, 70 vertical levels and hourly temporal resolution, offers a substantially better opportunity to identify cool-season tornadic environments. The BARRA team developed a climatology of low-level windshear over the southwest of WA, identifying regions with particularly high 95th percentile shear as being at greater risk of cool-season tornadogenesis than other parts of the BARRA-PH domain.

Typically, low-level windshear is calculated as the difference between the surface (10 m) wind and that at 1 or 1.5 km above the surface. Here, 1.5 km was used, and maximum daily values were calculated from the 24 hourly winds for each grid point in the domain (excluding edge regions distorted by boundary effects). Figure 2 shows BARRA-R (top row) and BARRA-PH (bottom row) plots of the 95th percentile of daily maximum low-level windshear over southwest WA, grouped by month, for January, April, July and October, as representative of austral summer, autumn, winter and spring, respectively. The windshear scale in each figure is m s^{-1}, and it is clear that the higher resolution model (BARRA-PH) resolves generally higher windshear values than BARRA-R over the domain. Of the months displayed, windshear values are lightest in April and substantially higher in July than in other months. This is unsurprising, given the exposure of southwest WA to winter storm systems and generally more settled conditions during autumn. For the same reason, values are highest on the south coast of WA. There is a pronounced peak in July about the far south coastal strip, likely reflecting coastal convergence of the generally westerly airstreams. A secondary peak in the same region occurs in January, but over coastal waters rather than land. This likely reflects the fact that the summertime boundary layer over land is more completely mixed than over water, thereby reducing overland windshears in comparison to those over adjacent waters. In BARRA-PH, the shoulder seasons do not display such a pronounced land–sea contrast, apart from at lighter windshear speeds, but there is some land–sea contrast evident at intermediate (20+ m s^{-1}) speeds within BARRA-R along parts of the WA south coast.

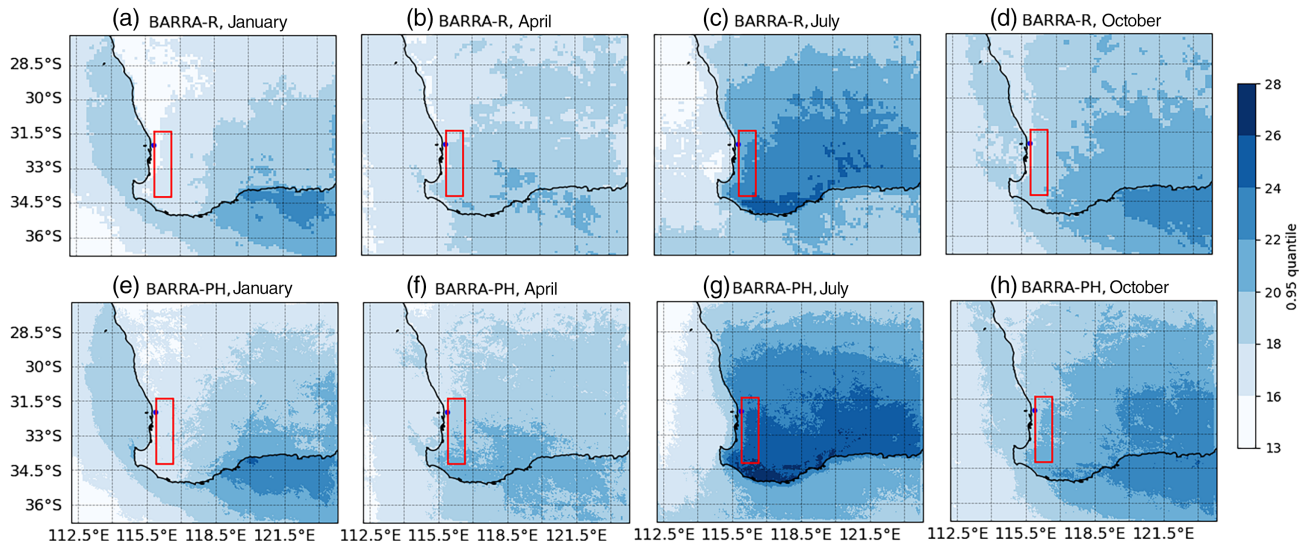

FIGURE 2 Plots of 95th percentile daily maximum windshear, in ms-1, grouped by representative season months, for southwest Western Australia. Top row is BARRA-R, bottom row is BARRA-PH. Region of Darling Escarpment is highlighted in red.

Also, evident in July, but to a lesser extent or not at all during other months, is a peak in windshear associated with the Darling Escarpment, running north–south inland of the coast in the far southwest.

The region of strongest low-level shear corresponds generally with the locations of reported cool-season tornadoes documented in Hanstrum et al. (2002). The greatest density of reports occurs, unsurprisingly, along the more heavily populated west coast of southwest WA, with fewer events documented on the far south coast. On the other hand, the region of highest low-level wind shear during July occurs along the less densely populated southern coast of WA. Notably, a broad area of southwestern WA is subject to shear comparable to that experienced in the area of highest frequency of reported cool-season tornadoes. This suggests that much of southwestern WA is subject to similar numbers of tornadoes as the densely populated, high-reporting area, a valuable insight derived from this dataset.

The current analysis considers only wind shear, noting that low-level atmospheric instability will contribute to tornado development in many cases. Nonetheless, this information provides useful information for WA emergency services to identify regions likely to be most at risk from cool-season tornadoes. As the name suggests, these phenomena are most common in winter, in regions where low-level windshear is high. The plots in Figure 2 identify such regions across the landscape and their seasonal variability, at a resolution that was not available prior to the development of BARRA-PH.

3.2 | Siting of portable AWS during periods of elevated fire danger

New South Wales Rural Fire Service (NSW RFS) approached the Bureau of Meteorology requesting assistance in deciding on optimal siting of portable Automated Weather Stations (AWS) during elevated fire danger situations and during ongoing fire activity to support operational decision-making. This study identified regions within the existing AWS network (Figure 3) where the information captured by the operational network is insufficient. These network 'gaps' may be the result of large distances between AWS or rapid changes in meteorological conditions associated with complex topography.

The McArthur Forest Fire Danger Index (FFDI, McArthur, 1967, Noble et al., 1980) is used in forested areas of eastern Australia to indicate levels of potential fire activity, with this index representing a combination of several near-surface weather conditions known to influence fire behaviour (based on measures of relative humidity, temperature, 10-min average wind speed and rainfall). The study of these fire weather conditions based on FFDI was conducted soon after the first tranche of 6 years of data for BARRA-SY became available, and thus extended for the period 1 January 2010 through 31 December 2015, rather than the entire BARRA-SY time frame of 1990 to 2019.

This study of the fire weather aspects produced a series of geographical information system layers to assist fire managers in deciding on the optimal siting of portable AWS across the state of New South Wales to fill gaps within the existing AWS network. One such layer is presented in Figure 4.

To identify gaps within the network, the FFDI time series at each reanalysis grid cell was correlated with the FFDI time series at the reanalysis grid cell corresponding to the location of the closest automated weather station. Pearson R correlation was used in this analysis as the fire agency was interested primarily in how a given location varied in comparison with the nearest AWS, rather than in estimates of absolute bias, which will not be detected using this method. Further, as a check, daily-resolved BARRA-R results were comparable to those from hourly-resolved BARRA-SY, indicating that the diurnal cycle did not substantially affect the results obtained using the higher resolution BARRA-SY. The results of this analysis are presented in Figure 4.

Figure 4 may be interpreted as follows: for a location where the Pearson R correlation coefficient is high, indicated by the cooler shading, the FFDI is strongly correlated with the FFDI at the closest automated weather station. The reverse is true for regions with weaker correlation coefficients, indicated by warmer shading. The weakest correlations (i.e., perceived gaps in the AWS network) in Figure 4 are found to coincide with the regions of particularly steep/complex topography (Figure 3) and are indicated in red. At these locations, the BARRA analysis indicates that the nearest AWS provides a poor representation of the local fire danger.

To assist in the interpretation of Figure 4, two additional sets of GIS layers were also created: spatial maps of the distance to the nearest automated weather station and the gradient of the topography (not shown here). These data layers assist the NSW RFS to deploy portable AWS to derive maximum benefit from the information that they provide, filling gaps in the network of permanent AWS when fires are anticipated or are occurring in the landscape.

Note that all GIS layers produced in the study were created using BARRA data. That is, the time series of FFDI at the location of each AWS was also derived from BARRA, rather than using the actual observations captured by the AWS. This approach has two immediate benefits:

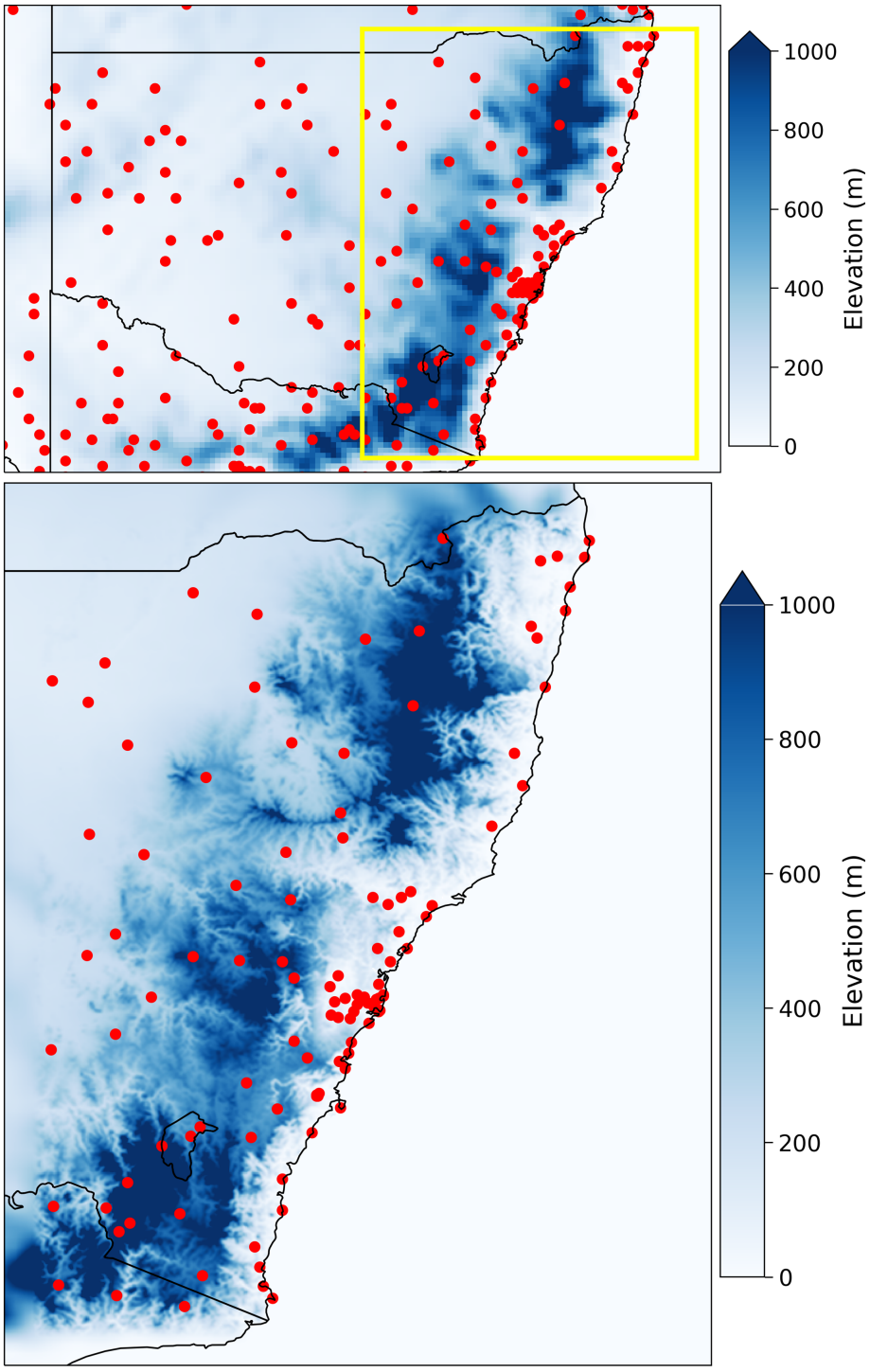

FIGURE 3 Model topography for the BARRA-R domain over New South Wales (~12 km grid resolution; top image) and the BARRA-SY subdomain (~1.5 km grid resolution; bottom image). The extent of the BARRA-SY domain is identified by the yellow border in the top image. The red markers identify the location of operational stations within the Bureau of Meteorology's Automated Weather Station Network.

1. The BARRA dataset provides a continuous and complete record of FFDI for 1 January 2010–31 December 2015. Actual AWS records can be subject to periods of outages (missing data) and may not have been operating for the entire study period.
2. The use of a single dataset (BARRA) reduces the influence of any biases that may exist between BARRA and actual observations (as noted above, the Pearson R coefficient will not detect such bias). Given this approach, no specific testing of bias between BARRA and AWS data was done, but as noted earlier, BARRA does contain a number of biases that would likely influence a comparison to AWS observations.

The study allowed a simple and objective assessment of the most cost-effective locations to site portable AWS, particularly during periods of elevated fire danger or

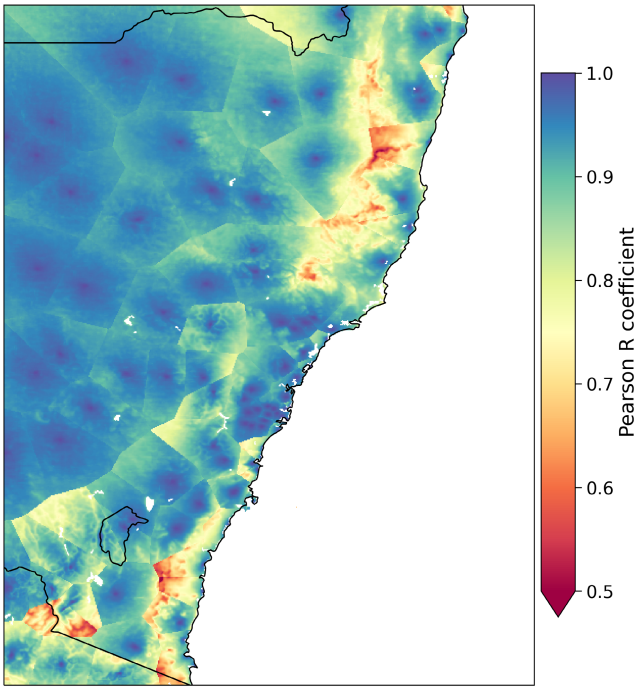

FIGURE 4 Map of the Pearson R correlation coefficient over the BARRA-SY subdomain showing how correlated the Forest Fire Danger Index (FFDI) is at a given location with the FFDI at the location of the nearest automated weather station

ongoing fires. In such circumstances, rapid but defensible decisions on resource deployment are required. This work assisted substantially in that regard. It would be interesting and useful to repeat this analysis with the entire (1990–2019) BARRA dataset, however resource constraints have not permitted this to date.

3.3 | Thunderstorm climatology and severe convective weather hazards

BARRA data have been useful in analysis for a variety of severe weather applications, including for examinations of thunderstorm-related hazards such as severe convective wind gusts (Brown & Dowdy, 2021), lightning and hail (Dowdy et al., 2020). As described earlier, the comprehensive coverage of a spatial domain offered by a reanalysis ensures that regions particularly subject to severe weather can be identified in any analysis, even when no surface observations are available. In particular, the use of a high-resolution reanalysis such as BARRA increases the likelihood that all such regions are identified despite the mesoscale variability in the occurrence of severe thunderstorms especially. Severe weather applications using BARRA have included the use of environmental diagnostics calculated from BARRA, such as measures commonly used in severe weather forecasting applications in the Australian Bureau of Meteorology as well as in other agencies such as the Storm Prediction Centre (SPC) from the U.S. National Oceanic and Atmospheric Administration (NOAA). Some examples of these environmental diagnostics include various measures based on CAPE, vertical wind shear, freezing level height as well as indices such as the significant hail parameter (SHIP; following the formulation used in NOAA https://www.spc.noaa.gov/exper/mesoanalysis/help/help_sigh.html). Examples of such applications are described in this section.

Figure 5 presents average values of CAPE for the period 1990–2018 mapped through Australia from BARRA and ERA5 reanalyses. The results for BARRA are broadly similar to those for ERA5, with some regional variations such as higher values for BARRA than ERA5 over the Southern Ocean and along parts of the densely populated eastern seaboard. A comparison with observations data at four locations is also presented using histograms of CAPE values. Those results show a good match between the reanalysis data and the observations-based data. This includes the higher values of CAPE, particularly in the case of BARRA, noting that these higher values of CAPE can be associated with the occurrence of severe thunderstorms and convective hazards.

BARRA data were used to examine environmental diagnostics for indicating the occurrence of lightning and hail, including for conditions averaged over many locations around Australia, as presented in Dowdy et al. (2020). This is also possible for individual locations, as presented here in Figure 6, demonstrating the use of BARRA for more specific guidance at a given location, in this case, for Brisbane in subtropical eastern Australia. These results are based on lightning observations from the World Wide Lightning Location Network of ground-based sensors (Virts et al., 2013.) and hail inferences from radar data, with further details on data and methods available in Dowdy et al. (2020). This shows that the BARRA environmental conditions provide a skilful means of distinguishing between the occurrence and non-occurrence of these thunderstorm hazards for this individual location. These results demonstrate features specific to the time of year and time of day, which could also be useful guidance for severe weather and hazard forecasting, noting that the BARRA reanalysis framework is very similar in many ways to the ACCESS system used operationally for weather forecasting in the Bureau of Meteorology (as detailed in sections above). Similar figures to this shown here for Brisbane (Figure 6) are also available on request from the authors for other locations around Australia, including capital cities and several regional cities.

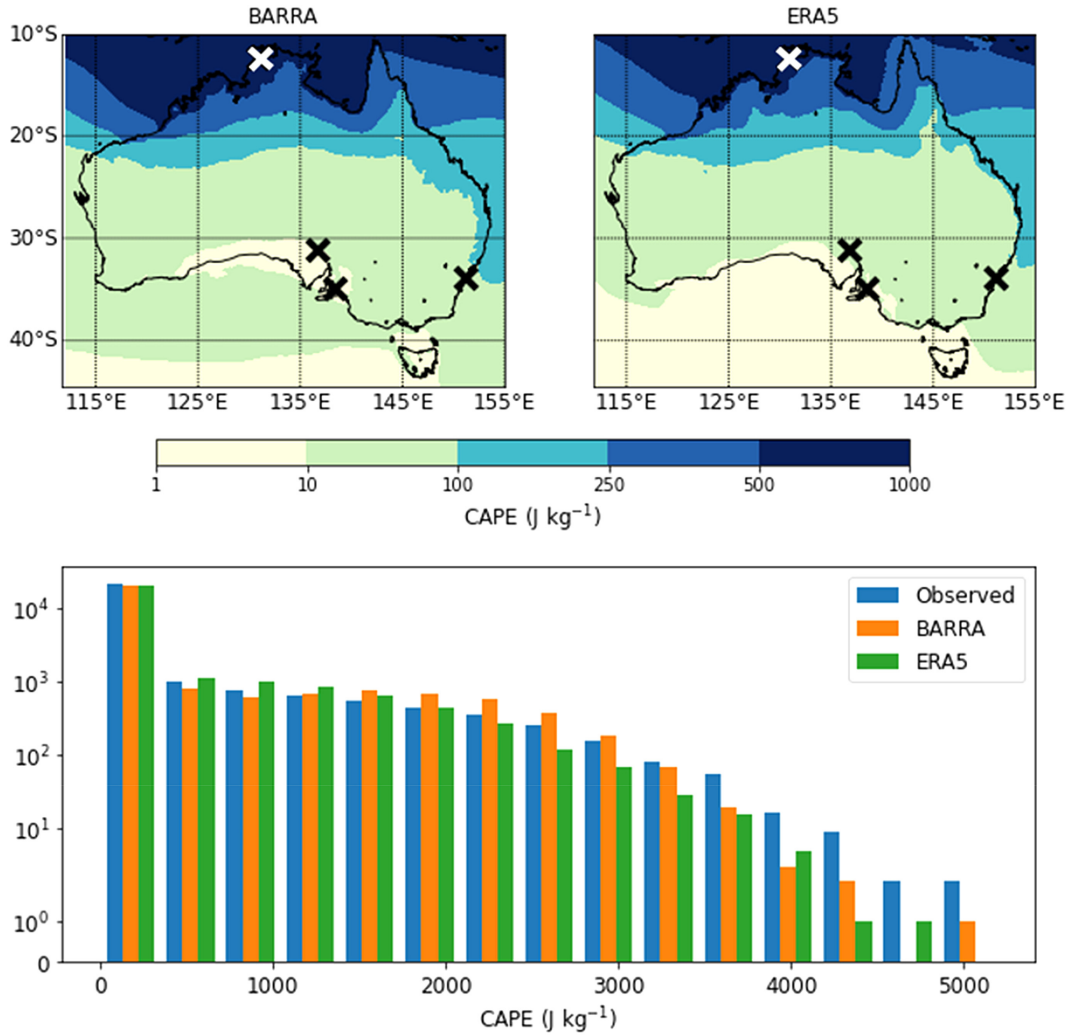

FIGURE 5 Spatial distribution of mean convective available potential energy (CAPE) from hourly instantaneous BARRA-R and ERA5 data from 1990 to 2018 (top panels), and a frequency distribution of reanalysis CAPE values compared with CAPE values derived from collocated (once to three times daily) rawinsonde observations (bottom panel). CAPE observations and collocated model values are from four locations, represented by crosses in the top figure panels (Adelaide, Darwin, Sydney and Woomera).

3.4 | Design rainfall applications

The statistical analysis of extreme rainfalls is generally used for design of hydraulic structures such as highways, urban drainage networks and dams. Such rainfalls are often presented in the form of intensity–duration–frequency (IDF) curves, also termed as 'design rainfall' (Chow et al., 1988). The design rainfalls are usually derived for varying durations ranging from sub-hourly up to 7 days, and in Australia, these are derived by fitting the generalized extreme value distribution to rainfall maxima obtained from both daily-read and pluviograph gauges (Green et al., 2019). The observation datasets that are required to derive such design rainfall estimates are often limited due to uneven and sparse spatial coverage, and shorter and inconsistent record lengths, and hence it is of interest to determine whether data from regional reanalysis (BARRA-R) can be used to derive design rainfalls in regions where there is a paucity of observations.

The assessment of design rainfalls derived from reanalysis across a larger domain is generally confounded by limited observations, particularly in mountainous areas. The Gold Coast region represents one of the more challenging and consequential regions in Australia for estimating IDF curves as it includes extensive urban development along a narrow coastal plain that is bordered to the west by the Great Dividing Range. The area includes the Gold Coast City (the sixth largest city in Australia, comprising around 670,000 people), which stretches approximately 50 km along the coast and 10 km inland, located 70 km south of Queensland's capital city, Brisbane. The hinterland to the west of the Gold Coast rises steeply to elevations of up to 1100 m. The region experiences a humid sub-tropical climate (Peel et al.,

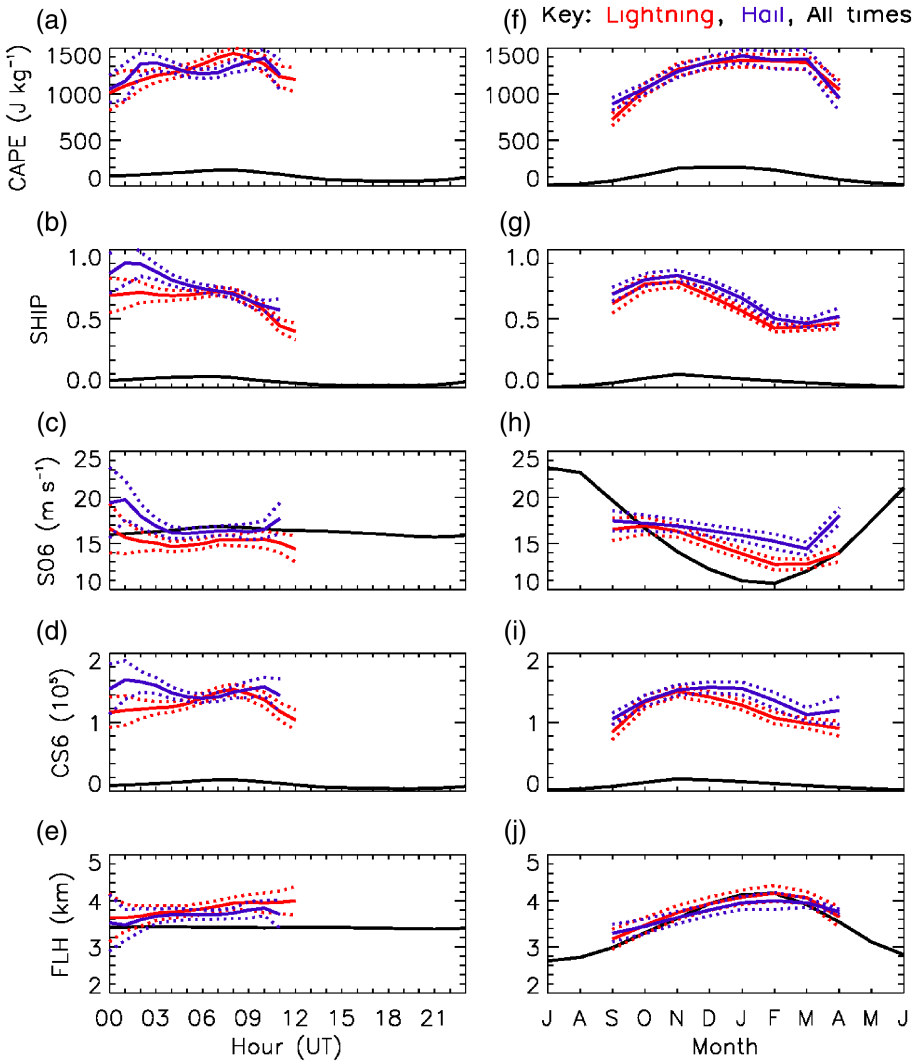

FIGURE 6 Environmental diagnostics from BARRA associated with observed lightning activity and radar-based hail data in Brisbane. Five environmental diagnostics are shown (convective available potential energy—CAPE: (a, f); significant hail parameter—SHIP: (b, g); bulk wind shear from 0 to 6 km—S06: (c, h); a product of CAPE and S06—CS6: (d, i); and freezing level height—FLH: (e, j) based on BARRA reanalysis data from 2005 to 2018. Average values are presented at the time of hail (blue) and lightning (red) occurrences, as well as for all time steps (black), presented for each hour (a–e) and month (f–j). This averaging includes ±1 time step for each value shown (i.e., ±1 h for the hourly information and ±1 month for the monthly results), with results shown only if at least 15 values contribute to a given average value. A confidence range is also indicated, based on showing one SE of the mean above and below the results (dotted lines).

2007), where precipitation mostly occurs in summer in thunderstorms and heavy showers. The region is served by a high density of sub-daily pluviograph gauges (compared to most other regions in Australia), and thus provides a useful benchmark for evaluation of design rainfall derived from BARRA-R.

The design rainfall estimates for the Gold Coast were derived by the Bureau of Meteorology using procedures described by Green et al. (2019). The process involved fitting a generalized extreme value distribution by L-Moments (Hosking & Wallis, 1997) to observed annual maxima, and the parameter values were then derived for gridded locations across the region using thin-plate smoothing splines; elevation was included as a covariate to help explain the systematic variation of design rainfalls with topography. The analysis for the Gold Coast region was undertaken using 48 high-quality gauges with more than 8 years of record. The corresponding design rainfall estimates obtained using the BARRA-R reanalysis data were derived by fitting a general extreme value distribution to the annual maxima series extracted from each grid cell.

A comparison of design rainfall estimates obtained from the two data sets is shown in Figure 7a,b, for a rainfall burst duration of 24 h and an annual exceedance probability (AEP) of 1% (i.e., a recurrence interval of 100 years). It is seen that the overall spatial pattern of the 1% AEP design rainfalls obtained using BARRA-R is similar to those based on gauged data; however, the spatial variability in the BARRA-R estimates is higher compared with the gridded estimates based on gauged point rainfalls. Results for all sub-daily durations for an AEP of 1% are summarized in Figure 7c. The differences in spatial variability between the two sets of estimates are evident in the widths of the shaded regions, where again it is seen that estimates based on BARRA-R are generally more variable than those based on gauged data. It is also evident that the BARRA-R design rainfall estimates are higher than those based on gauged data. It needs to be recognized that both sets of gridded design rainfalls

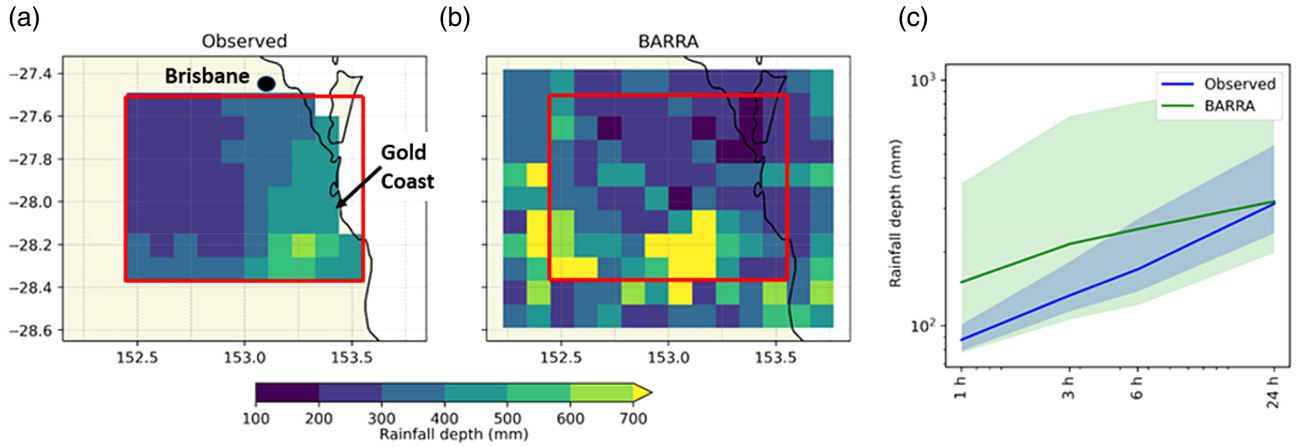

FIGURE 7 Design rainfall estimates for 24 h duration and 1% annual exceedance probability (AEP) based on (a) gauged observations and (b) BARRA-R rainfall. Panel (c) summarizes the differences in results for all sub-daily durations for an AEP of 1%, where the solid line and the shaded region respectively represent the median design depth and the 5%–95% range of design depths over the selected region. A red box in panels (a) and (b) covers identical areas and is included for ease of comparison.

involve assumptions, and that the estimates based on gauged data cannot be regarded as the 'true' value as they involve the additional step of using thin-plate splines to fit a surface of gridded design rainfalls based on point gauge locations. Overall, the nature of these differences in gridded design rainfalls is consistent with the evaluation of point-to-grid rainfall frequency presented in Acharya et al. (2020).

While there are appreciable differences in the estimates of sub-daily design rainfalls across the region based on BARRA-R and gauged data, there are many regions in Australia that are poorly served by rainfall gauges, which would benefit from the availability of BARRA-R data. The potential to which reanalysis products can be used to provide direct estimates of design rainfalls, or else be used as a covariate to help inform the spatial interpolation between gauged locations, thus remains an active area of research. It is also worth noting that information on the spatio-temporal patterns of rainfalls (which are required to be specified when inputting design rainfalls into hydrologic models) over meso-scales relevant to catchment hydrology is another area of ongoing investigation, particularly for sub-daily durations relevant to the estimate of flood risks (Acharya et al., 2020).

4 | DISCUSSION AND CONCLUSIONS

We have presented brief summaries of several applications of the BARRA reanalysis dataset, each having an emergency management focus. Compared with global reanalyses, high-resolution BARRA reanalyses offer the advantage that better-resolved topography and atmospheric processes improve understanding of potential impacts of weather and climate phenomena. This is because the higher, kilometre-scale resolution is closer to the scale at which emergency services observe, plan for and respond to events. Compared with observational datasets, the comprehensive coverage of a domain offered by regional reanalyses ensures that areas of potential emergency management concern, including fire, heavy precipitation or severe thunderstorm hazards, can be represented in population and asset risk assessments.

We have discussed a small, generally representative selection of applications of BARRA, to illustrate its applicability to assist with emergency management problems. Topics not included above but which have received at least preliminary attention include development of climatology of the new Australian Fire Danger Rating System (Matthews et al., 2019). Such a climatology is valuable to calibrate and better understand the performance of the new system, and to identify thresholds for alerting for particular quantities such as wind change strength (Mills et al., 2020) and continuous Haines Index (Mills & McCaw, 2010). The high temporal resolution also permits investigation of changes in fire danger as a result of the diurnal cycle. Earlier work (Fox-Hughes, 2011) used observations at widely spaced automatic weather station locations in preliminary investigations, but landscape-wide analysis was not possible. The high spatial and temporal resolution of the BARRA regional reanalysis now permits closer investigation of changes in diurnality, particularly with elevation given the ability of the reanalysis to resolve topographical features in considerable detail. A number of fire agencies are also using BARRA data to update planning regimes, which are based on estimated fire danger return periods. Aside from fire applications, BARRA has been used in identification of coastal waters

regions subject to strong wind, and to highlight locations subject to enhanced winds generally, particularly from unusual wind directions (Fox-Hughes et al., 2019). It has also been applied, with ERA5 reanalysis (Hersbach et al., 2020), to the investigation of tropical cyclone wind gusts in the Australian region, including any changes that have occurred in tropical cyclone-related gust strength (Bell et al., 2021).

While we have discussed climatologies or similar applications because they offer broad-ranging immediate benefits, there is in addition very considerable potential to study individual case studies with an emergency management focus. Important examples include convective flood events, even if the model underpinning the reanalysis does not fully resolve fine detail of the training of convective cell over locations (Malguzzi et al., 2006; Senatore et al., 2020). Regional reanalyses have additionally provided valuable insights into fire events (Huang et al., 2009, using North American Regional Reanalysis as the boundary conditions for further downscaling, Ndalila et al., 2020) and extreme wind events (Fox-Hughes et al., 2018; Richter et al., 2019). Smaller-scale case studies such as these and others can offer very valuable insights into the typical behaviour of the atmosphere in high-impact or high-value situations.

We have not considered other applications besides those focussed on emergency management. There are many direct meteorological or climatological applications of regional reanalyses, of course, but here we have focussed on applications outside these fields. Renewable energy research makes extensive use of regional reanalyses to identify locations with optimal energy generation prospects, including steady reliable wind and frequent sunny conditions (Ashtine et al., 2016; Camargo et al., 2019; Frank et al., 2018; Holt & Wang, 2012). Several such studies are underway or have been conducted in Australia using BARRA. Agricultural (Lu et al., 2019) and ecological applications also take advantage of the high spatial and temporal resolution of regional reanalyses to investigate the location-dependent response of living systems to weather and climate conditions.

Future implementations of high-resolution reanalyses in the Australian region are being considered currently. These may include additional high-resolution domains to those currently existing. In addition, the period covered by BARRA may be extended further into the past, to 1980. Bias correction of some quantities is under consideration, particularly wind speed, given its importance for emergency management (e.g., for input to fire weather measures such as the Forest Fire Danger Index) and renewable energy applications (e.g., for applications associated with wind turbines). Finally, uncertainty estimates may be quantified by the development of an ensemble of reanalysis products, noting the potential for this to be considered for subsequent versions of BARRA as part of scope for future development activities.

AUTHOR CONTRIBUTIONS

Paul Fox-Hughes: Conceptualization (equal); funding acquisition (equal); investigation (equal); writing – original draft (lead); writing – review and editing (lead). **Chun-Hsu Su:** Conceptualization (equal); data curation (equal); investigation (lead); software (lead); writing – original draft (equal). **Nathan Eizenberg:** Data curation (equal); investigation (equal); software (equal); writing – review and editing (supporting). **Christopher J. White:** Conceptualization (equal); funding acquisition (equal); writing – review and editing (equal). **Peter Steinle:** Data curation (equal); investigation (equal); software (equal); supervision (equal). **Doerte Jakob:** Conceptualization (equal); data curation (equal); investigation (equal); supervision (equal); writing – original draft (equal). **Mitchell Black:** Investigation (equal); software (equal); writing – original draft (equal). **Andrew Dowdy:** Investigation (equal); supervision (equal); writing – original draft (equal). **Andrew Brown:** Investigation (equal); software (equal); writing – original draft (equal). **Rory Nathan:** Investigation (equal); supervision (equal); writing – original draft (equal). **Suwash Chandra Acharya:** Investigation (equal); software (equal); writing – original draft (equal).

ACKNOWLEDGEMENT

The authors thank the anonymous reviewers for their helpful suggestions, which improved the content and appearance of the manuscript.

FUNDING INFORMATION

Australian emergency management agencies provided funding to undertake this work: New South Wales Rural Fire Service, West Australian Department of Fire and Emergency Services, South Australian Department of Environment and Water and Country Fire Service. In addition, funding from Tasmania was supported by the Tasmanian and Australian Governments, under the Tasmanian Bushfire Mitigation Grants Program together with the Antarctic Climate and Ecosystems Co-operative Research Centre and University of Tasmania. Many colleagues at the Bureau of Meteorology contributed to the development of BARRA, as did colleagues at the United Kingdom Met Office, ECMWF and New Zealand National Institute of Water and Atmospheric Research. This research/project was undertaken with the assistance of resources and services from the National Computational Infrastructure (NCI), which is supported by the Australian Government.

CONFLICT OF INTEREST

The authors declare no conflict of interest.

DATA AVAILABILITY STATEMENT

BARRA data are available through: https://dapds00.nci.org.au/thredds/catalogs/cj37/catalog.html.

ORCID

Paul Fox-Hughes https://orcid.org/0000-0002-0083-9928
Peter Steinle https://orcid.org/0000-0002-0996-3386

REFERENCES

Abatzoglou, J.T., Hatchett, B.J., Fox-Hughes, P., Gershunov, A. & Nauslar, N.J. (2021) Global climatology of synoptically-forced downslope winds. *International Journal of Climatology*, 41(1), 31–50.

Acharya, S.C., Nathan, R., Wang, Q.J., Su, C.-H. & Eizenberg, N. (2019) An evaluation of daily precipitation from a regional atmospheric reanalysis over Australia. *Hydrology and Earth System Sciences*, 23, 3387–3403. https://doi.org/10.5194/hess-23-3387-2019

Acharya, S.C., Nathan, R., Wang, Q.J., Su, C.-H. & Eizenberg, N. (2020) Ability of an Australian reanalysis dataset to characterise sub-daily precipitation. *Hydrology and Earth System Sciences*, 24, 2951–2962. https://doi.org/10.5194/hess-24-2951-2020

Ashrit, R., Indira Rani, S., Kumar, S., Karunasagar, S., Arulalan, T., Francis, T. et al. (2020) IMDAA regional reanalysis: performance evaluation during Indian summer monsoon season. *Journal of Geophysical Research-Atmospheres*, 125(2), e2019JD030973.

Ashtine, M., Bello, R. & Higuchi, K. (2016) Assessment of wind energy potential over Ontario and Great Lakes using the NARR data: 1980–2012. *Renewable and Sustainable Energy Reviews*, 56, 272–282.

Bell, S., Chand, S., Dowdy, A., Ramsay, H., Deo, A., Su, C.-H. et al. (2021) *Australian tropical cyclone-induced extreme coastal winds in climate datasets*. Bureau of Meteorology Research Report 56. ISBN 978-1-925738-31-5. Available at: http://www.bom.gov.au/research/publications/researchreports/BRR-056.pdf [Accessed August 02, 2022].

Best, M.J., Pryor, M., Clark, D.B., Rooney, G.G., Essery, R.L.H., Ménard, C.B. et al. (2011) The Joint UK Land Environment Simulator (JULES), model description – part 1: energy and water fluxes. *Geoscientific Model Development*, 4, 677–699. https://doi.org/10.5194/gmd-4-677-2011

Bollmeyer, C., Keller, J.D., Ohlwein, C., Wahl, S., Crewell, S., Friederichs, P. et al. (2015) Towards a high-resolution regional reanalysis for the European CORDEX domain. *Quarterly Journal of the Royal Meteorological Society*, 141(686), 1–15.

Bromwich, D.H., Wilson, A.B., Bai, L.S., Moore, G.W. & Bauer, P. (2016) A comparison of the regional Arctic system reanalysis and the global ERA-Interim Reanalysis for the Arctic. *Quarterly Journal of the Royal Meteorological Society*, 142(695), 644–658.

Brooks, H.E., Lee, J.W. & Craven, J.P. (2003) The spatial distribution of severe thunderstorm and tornado environments from global reanalysis data. *Atmospheric Research*, 67, 73–94.

Brown, A. & Dowdy, A. (2021) Severe convection-related winds in Australia and their associated environments. *Journal of Southern Hemisphere Earth Systems Science*, 71, 30–52.

Bureau of Meteorology. (2018) *APS2 upgrade of the ACCESS-C numerical weather prediction system*. National Operational Centre Operations Bulletin No. 114. Available at: http://www.bom.gov.au/australia/charts/bulletins/BNOC_Operations_Bulletin_114.pdf [Accessed 12th December 2020].

Bureau of Meteorology. (2019) *APS3 upgrade of the ACCESS-G/GE numerical weather prediction system*. National Operational Centre Operations Bulletin No. 125. Available at: http://www.bom.gov.au/australia/charts/bulletins/opsbull_G3GE3_external_v3.pdf [Accessed 12th December 2020].

Camargo, L.R., Gruber, K. & Nitsch, F. (2019) Assessing variables of regional reanalysis data sets relevant for modelling small-scale renewable energy systems. *Renewable Energy*, 133, 1468–1478.

Cardinali, C. (2013) Observation influence diagnostic of a data assimilation system. In: *Data assimilation for atmospheric, oceanic and hydrologic applications*, Vol. II. Berlin, Heidelberg: Springer, pp. 89–110.

Chow, V.T., Maidment, D.R. & Mays, L.W. (1988) *Applied hydrology*. New York, NY: McGraw-Hill.

Clark, M.R. (2009) The southern England tornadoes of 30 December 2006: case study of a tornadic storm in a low CAPE, high shear environment. *Atmospheric Research*, 93(1–3), 50–65.

Courtier, P., Thépaut, J.-N. & Hollingsworth, A. (1994) A strategy for operational implementation of 4D-Var, using an incremental approach. *Quarterly Journal of the Royal Meteorological Society*, 120, 1367–1387. https://doi.org/10.1002/qj.49712051912

Davies, T., Cullen, M.J.P., Malcolm, A.J., Mawson, M.H., Staniforth, A., White, A.A. et al. (2005) A new dynamical core for the Met Office's global and regional modelling of the atmosphere. *Quarterly Journal of the Royal Meteorological Society*, 131, 1759–1782. https://doi.org/10.1256/qj.04.101

Dee, D.P., Uppala, S.M., Simmons, A.J., Berrisford, P., Poli, P., Kobayashi, S. et al. (2011) The ERA-Interim reanalysis: configuration and performance of the data assimilation system. *Quarterly Journal of the Royal Meteorological Society*, 137(656), 553–597.

Diniz, F.L. & Todling, R. (2020) Assessing the impact of observations in a multi-year reanalysis. *Quarterly Journal of the Royal Meteorological Society*, 146(727), 724–747.

Dowdy, A.J., Soderholm, J., Brook, J., Brown, A. & McGowan, H. (2020) Quantifying hail and lightning risk factors using long-term observations around Australia. *Journal of Geophysical Research-Atmospheres*, 125, 2020JD033101.

Fox-Hughes, P. (2011) Impact of more frequent observations on the understanding of Tasmanian fire danger. *Journal of Applied Meteorology and Climatology*, 50(8), 1617–1626.

Fox-Hughes, P., Bally, J. & Hubbert, G. (1996) A tornadic thunderstorm in northwest Tasmania: 22 November 1992. *Australian Meteorological Magazine*, 45, 161–175.

Fox-Hughes, P., Barnes-Keoghan, I. & Porter, A. (2018) Observations of a tornado at an automatic Weather Station in northern Tasmania. *Journal of Southern Hemisphere Earth Systems Science*, 68(1), 215–230.

Fox-Hughes, P., Sauvage, S., Su, C.-H., Eizenberg, N., Jakob, D., White, C. et al. (2019) A high-resolution gridded wind dataset

for Tasmania using BARRA. *Proceedings of the Australian Meteorological and Oceanographic Society Annual Meeting, Darwin, Australia*.

Frank, C.W., Wahl, S., Keller, J.D., Pospichal, B., Hense, A. & Crewell, S. (2018) Bias correction of a novel European reanalysis data set for solar energy applications. *Solar Energy*, 164, 12–24.

Giese, B.S., Compo, G.P., Slowey, N.C., Sardeshmukh, P.D., Carton, J.A., Ray, S. et al. (2010) The 1918/19 El Niño. *Bulletin of the American Meteorological Society*, 91(2), 177–183.

Gleeson, E., Whelan, E. & Hanley, J. (2017) Met Éireann high resolution reanalysis for Ireland. *Advances in Science and Research*, 14, 49–61.

Green, J., Johnson, F., Beesley, C. & The, C. (2019) Chapter 3—design rainfall. In: Ball, J., Babister, M., Nathan, R., Weeks, W., Weinmann, E., Retallick, M. et al. (Eds.) *Australian rainfall and runoff: a guide to flood estimation*. Australia: Commonwealth of Australia (Geosciences Australia).

Grumm, R.H., Ross, J.D. & Knight, P.G. (2005) *Examining severe weather events using reanalysis datasets*. Preprints, 21st Conf. on Weather Analysis and Forecasting/17th Conf. on Numerical Weather Prediction, Washington, DC, Amer. Meteor. Soc., CD-ROM, P1.87.

Hamill, T.M., Schneider, R.S., Brooks, H.E., Forbes, G.S., Bluestein, H.B., Steinberg, M. et al. (2005) The May 2003 extended tornado outbreak. *Bulletin of the American Meteorological Society*, 86(4), 531–542.

Hanstrum, B.N., Mills, G.A., Watson, A., Monteverdi, J.P. & Doswell, C.A., III. (2002) The cool-season tornadoes of California and southern Australia. *Weather and Forecasting*, 17(4), 705–722.

Hersbach, H., Bell, B., Berrisford, P., Hirahara, S., Horányi, A., Muñoz-Sabater, J. et al. (2020) The ERA5 global reanalysis. *Quarterly Journal of the Royal Meteorological Society*, 146(730), 1999–2049. https://doi.org/10.1002/qj.3803

Holt, E. & Wang, J. (2012) Trends in wind speed at wind turbine height of 80 m over the contiguous United States using the North American Regional Reanalysis (NARR). *Journal of Applied Meteorology and Climatology*, 51(12), 2188–2202.

Hosking, J.R.M. & Wallis, J.R. (1997) *Regional frequency analysis: an approach based on L-moments*. Cambridge: Cambridge University Press.

Huang, C., Lin, Y.L., Kaplan, M.L. & Charney, J.J. (2009) Synoptic-scale and mesoscale environments conducive to forest fires during the October 2003 extreme fire event in Southern California. *Journal of Applied Meteorology and Climatology*, 48(3), 553–579.

Jakob, D., Su, C.-H., Eizenberg, N., Kociuba, G., Steinle, P., Fox-Hughes, P. et al. (2017) An atmospheric high-resolution regional reanalysis for Australia. *The Bulletin of the Australian Meteorological and Oceanographic Society*, 30, 16–23.

Kaiser-Weiss, A.K., Borsche, M., Niermann, D., Kaspar, F., Lussana, C., Isotta, F.A. et al. (2019) Added value of regional reanalyses for climatological applications. *Environmental Research Communications*, 1(7), 071004.

King, J.R., Parker, M.D., Sherburn, K.D. & Lackmann, G.M. (2017) Rapid evolution of cool season, low-CAPE severe thunderstorm environments. *Weather and Forecasting*, 32(2), 763–779.

Kounkou, R., Mills, G. & Timbal, B. (2009) A reanalysis climatology of cool-season tornado environments over southern Australia. *International Journal of Climatology: A Journal of the Royal Meteorological Society*, 29(14), 2079–2090.

Leitão, P. & Pinto, P. (2020) Tornadoes in Portugal: an overview. *Atmosphere*, 11(7), 679. https://doi.org/10.3390/atmos11070679

Lu, J., Carbone, G.J. & Gao, P. (2019) Mapping the agricultural drought based on the long-term AVHRR NDVI and North American Regional Reanalysis (NARR) in the United States, 1981–2013. *Applied Geography*, 104, 10–20.

Malguzzi, P., Grossi, G., Buzzi, A., Ranzi, R. & Buizza, R. (2006) The 1966 "century" flood in Italy: a meteorological and hydrological revisitation. *Journal of Geophysical Research-Atmospheres*, 111(D24106). https://doi.org/10.1029/2006JD007111

Manney, G.L. & Hegglin, M.I. (2018) Seasonal and regional variations of long-term changes in upper-tropospheric jets from reanalyses. *Journal of Climate*, 31(1), 423–448.

Matthews, S., Fox-Hughes, P., Grootemaat, S., Hollis, J.J., Kenny, B. J. & Sauvage, S. (2019) *Australian fire danger rating system: research prototype*. Lidcombe: NSW Rural Fire Service, p. 384.

May, P., Trewin, B., Su, C.-H. & Ostendorf, B. (2021) Verification of moist surface variables over northern Australia in a high resolution reanalysis (BARRA). *Journal of Southern Hemisphere Earth Systems Science*, 71(2), 194–202.

McArthur, A.G. (1967) *Fire behaviour in eucalypt forests*. Leaflet no. 107. Canberra: Forestry and Timber Bureau, p. 25.

Mesinger, F., DiMego, G., Kalnay, E., Mitchell, K., Shafran, P.C., Ebisuzaki, W. et al. (2006) North American regional reanalysis. *Bulletin of the American Meteorological Society*, 87(3), 343–360.

Mills, G.A. (2005) A re-examination of the synoptic and mesoscale meteorology of Ash Wednesday 1983. *Australian Meteorological Magazine*, 54(1), 35–55.

Mills, G.A. (2004) Verification of operational cool-season tornado threat-area forecasts from mesoscale NWP and a probabilistic forecast product. *Australian Meteorological Magazine*, 53(4), 269–277.

Mills, G.A., Harris, S., Brown, T. & Chen, A. (2020) Climatology of wind changes and elevated fire danger over Victoria, Australia. *Journal of Southern Hemisphere Earth Systems Science*, 70, 290–303. https://doi.org/10.1071/ES19043

Mills, G.A. & McCaw, W.L. (2010) *Atmospheric stability environments and fire weather in Australia: extending the Haines Index*. CAWCR Technical Report 20, CSIRO and Bureau of Meteorology, Victoria, p. 158.

Monteverdi, J.P. & Quadros, J. (1994) Convective and rotational parameters associated with three tornado episodes in northern and central California. *Weather and Forecasting*, 9(3), 285–300.

Ndalila, M.N., Williamson, G.J., Fox-Hughes, P., Sharples, J. & Bowman, D.M. (2020) Evolution of a pyrocumulonimbus event associated with an extreme wildfire in Tasmania, Australia. *Natural Hazards and Earth System Sciences*, 20(5), 1497–1511.

Neff, B., Kummli, C., Stickler, A., Franke, J. & Brönnimann, S. (2013) An analysis of the Galveston Hurricane using the 20CR data set. In: Brönnimann, S. & Martius, O. (Eds.) *Weather extremes during the past 140 years*, Vol. G89. Bern, Switzerland: Geographica Bernensia, pp. 27–34. https://doi.org/10.4480/GB2013.G89.03

Noble, I.R., Bary, G.A.V. & Gill, A.M. (1980) McArthur's fire-danger meters expressed as equations. *Australian Journal of Ecology*, 5, 201–203.

Peel, M.C., Finlayson, B.L. & McMahon, T.A. (2007) Updated world map of the Köppen-Geiger climate classification. *Hydrology and Earth System Sciences*, 11, 1633–1644. https://doi.org/10.5194/hess-11-1633-2007

Rawlins, F., Ballard, S.P., Bovis, K.J., Clayton, A.M., Li, D., Inverarity, G.W. et al. (2007) The Met Office global 4-dimensional data assimilation system. *Quarterly Journal of the Royal Meteorological Society*, 133, 347–362. https://doi.org/10.1002/qj.32

Richter, H., Arthur, C., Wehner, M., Wilke, D., Dunford, M. & Ebert, B. (2019) *The physical impact of strong winds and heavy rain on residential housing: a pilot study*. Bushfire and Natural Hazards CRC Research Day AFAC19, Melbourne, Australia.

Rodríguez, O. & Bech, J. (2021) Tornadic environments in the Iberian Peninsula and the Balearic Islands based on ERA5 reanalysis. *International Journal of Climatology*, 41, E1959–E1979.

Senatore, A., Davolio, S., Furnari, L. & Mendicino, G. (2020) Reconstructing flood events in Mediterranean coastal areas using different reanalyses and high-resolution meteorological models. *Journal of Hydrometeorology*, 21(8), 1865–1887.

Sherburn, K.D., Parker, M.D., King, J.R. & Lackmann, G.M. (2016) Composite environments of severe and nonsevere high-shear, low-CAPE convective events. *Weather and Forecasting*, 31(6), 1899–1927.

Škerlak, B., Sprenger, M., Pfahl, S., Tyrlis, E. & Wernli, H. (2015) Tropopause folds in ERA-Interim: global climatology and relation to extreme weather events. *Journal of Geophysical Research-Atmospheres*, 120(10), 4860–4877.

Slivinski, L.C., Compo, G.P., Sardeshmukh, P.D., Whitaker, J.S., McColl, C., Allan, R.J. et al. (2021) An evaluation of the performance of the twentieth century reanalysis version 3. *Journal of Climate*, 34(4), 1417–1438.

Stucki, P., Bandhauer, M., Heikkilä, U., Rössler, O., Zappa, M., Pfister, L. et al. (2018) Reconstruction and simulation of an extreme flood event in the Lago Maggiore catchment in 1868. *Natural Hazards and Earth System Sciences*, 18(10), 2717–2739.

Stucki, P., Brönnimann, S., Martius, O., Welker, C., Rickli, R., Dierer, S. et al. (2015) Dynamical downscaling and loss modeling for the reconstruction of historical weather extremes and their impacts: a severe Foehn storm in 1925. *Bulletin of the American Meteorological Society*, 96(8), 1233–1241.

Su, C.-H., Eizenberg, N., Jakob, D., Fox-Hughes, P., Steinle, P., White, C.J. et al. (2021) BARRA v1.0: kilometre-scale downscaling of an Australian regional atmospheric reanalysis over four midlatitude domains. *Geoscientific Model Development Discussion*, 14, 4357–4378. https://doi.org/10.5194/gmd-14-4357-2021

Su, C.-H., Eizenberg, N., Steinle, P., Jakob, D., Fox-Hughes, P., White, C.J. et al. (2019) BARRA v1.0: the Bureau of Meteorology Atmospheric high-resolution regional reanalysis for Australia. *Geoscientific Model Development*, 12, 2049–2068. https://doi.org/10.5194/gmd-12-2049-2019

Tyrrell, J. (2007) Winter tornadoes in Ireland: the case of the Athlone tornado of 12 January 2004. *Atmospheric Research*, 83(2–4), 242–253.

Virts, K.S., Wallace, J.M., Hutchins, M.L. & Holzworth, R.H. (2013) Highlights of a new ground-based, hourly global lightning climatology. *Bulletin of the American Meteorological Society*, 94, 1381–1391.

Viswanadhapalli, Y., Dasari, H.P., Langodan, S., Challa, V.S. & Hoteit, I. (2017) Climatic features of the Red Sea from a regional assimilative model. *International Journal of Climatology*, 37, 2563–2581. https://doi.org/10.1002/joc.4865

Wahl, S., Bollmeyer, C., Crewell, S., Figura, C., Friederichs, P., Hense, A. et al. (2017) A novel convective-scale regional reanalysis COSMO-REA2: improving the representation of precipitation. *Meteorologische Zeitschrift*, 26(4), 345–361.

Watson, A. (1985) *An examination of three winter tornadoes in southwest Western Australia*. Meteorological note 162. Melbourne: Bureau of Meteorology, Department of Sciences.

Yang, E.-G., Kim, H.M. & Kim, D.-H. (2022) Development of East Asia Regional Reanalysis based on advanced hybrid gain data assimilation method and evaluation with E3DVAR, ERA-5, and ERA-Interim reanalysis. *Earth System Science Data Discussions,* 14(4), 2109–2127. https://doi.org/10.5194/essd-2021-217

How to cite this article: Fox-Hughes, P., Su, C.-H., Eizenberg, N., White, C., Steinle, P., Jakob, D., Black, M., Dowdy, A., Brown, A., Nathan, R., & Acharya, S. C. (2022). A review of early severe weather applications of high-resolution regional reanalysis in Australia. *Meteorological Applications*, *29*(4), e2087. https://doi.org/10.1002/met.2087